Signed motif analysis of the *Caenorhabditis elegans* neuronal network reveals positive feedforward and negative feedback loops

Short title: Signed motif analysis of the Caenorhabditis elegans connectome

Gabor S. Szilagyi[1,2], Attila Gulyas[1], Zsolt Vassy[1], Peter Csermely[1], Bank G. Fenyves[1,3]

Affiliations:

1. Department of Molecular Biology, Semmelweis University, Budapest, Hungary
2. Department of Orthopaedics, Semmelweis University, Budapest, Hungary
3. Department of Emergency Medicine, Semmelweis University, Budapest, Hungary

Corresponding author: Bank G. Fenyves

Mail address: Ulloi ut 26, Budapest 1085, Hungary

Email: fenyves.bank@semmelweis.hu

KEYWORDS: connectome, feedforward excitation, feedback inhibition, feedback disinhibition, incoherent feedforward loop, biological switches, topology preserving randomization

Abstract

Nervous systems are complex biological networks with largely unknown structural and functional characteristics. Motif analysis is a robust tool that can reveal unique aspects of

connectivity of a complex network. An ideal candidate for motif analysis is the connectome of the nematode *Caenorhabditis elegans* which is the only fully reconstructed nervous system. Utilizing recent data on the connection signs of this network and a novel structure-preserving randomization method, we performed signed motif analysis on the *C. elegans* connectome for the first time, to our knowledge. We identified 56 significantly over- and 1 underrepresented three-node signed motifs and revealed that certain motifs (e.g. positive feedforward, negative feedback, disinhibitory feedback, and incoherent feedforward loops) are overabundant in the *C. elegans* connectome. We further distinguished (coloured) nodes by corresponding neuron modalities (e.g. sensory vs. motor neurons) and found that there is characteristic neuronal layout for each significant feedforward and feedback loop. Our findings demonstrate the importance and potential of signed motif analysis in understanding biological networks. Our motif enumerating tool and definition system can be utilized in signed motif analysis of other complex networks.

Introduction

Nervous systems are complex biological networks that generate behaviour *via* complex neural activity over the synaptic connectivity structure. Biological networks share common global (e.g. small-worldness, cost-efficient wiring) and local (e.g. clustering, modularization) properties that allow optimal information processing (1–4). Importantly, detailed structural characteristics can be revealed by investigating a network's composition from smaller building blocks, called motifs (Fig 1A). Motifs are frequently occurring subgraphs that correspond to different biological functions (3). A subgraph is a graph whose nodes and edges are subsets of another graph. There are two main types: induced and partial (5). A subgraph is induced if it has a subset of nodes of a network and all edges that connect those nodes. On the other hand, partial subgraphs only have some edges connecting the chosen

nodes (Fig 1B). The classical concept is that if a specific subgraph occurs in a network more frequently than expected then that subgraph might possess a crucial role in the network, hence is called a motif. Motifs have been examined in a variety of real-world and more importantly, brain networks (3,4,6). Similar to the networks themselves, motifs are primarily characterized by their nodes and edges.

Fig 1. Overview of motif definitions. A) Three-node motif structures with directed edges. B) Induced and partial motifs. Partial motifs are subgraphs of their corresponding induced motif. For example, induced motif E contains five different partial motifs. Similar concept is discussed in McDonnell *et al.* (2014) and Sporns & Kötter (2004). C) Definition of signed motifs by colouring the edges (of motif G in the example). An edge can be either excitatory or inhibitory.

Particularly in brain networks edges can be labelled ('coloured') by the polarity of the connection they represent – i.e. excitatory or inhibitory (Fig 1C). This is important as structurally identical motifs with different polarity patterns can have completely different biological functions. However, edge polarity-labelled (i.e. signed) motif analysis has only been performed in recent years (7,8) in social networks and partial connectomes, and has not been performed on a complete neuronal network yet. This is because large-scale polarity data has been lacking in most species.

The neuronal network of the nematode *Caenorhabditis elegans* is currently the only completely reconstructed connectome of a living organism's nervous system (9,10) consisting of 302 neurons and ~5000 connections in a hermaphrodite. In previous work on truncated and partial worm connectomes, some network motifs of three and four nodes were found to be overrepresented (3,9). More functional analyses have been performed in recent

studies which coloured the nodes based on neuronal function and neurotransmitter expression or labelled the edges by synapse type (11–13).

In a recent work we published a comprehensive dataset of synaptic polarities for the *C. elegans* chemical synapse connectome (14). Using presynaptic neurotransmitter and postsynaptic receptor expression data we predicted the polarities (excitatory, inhibitory, or complex) of more than 15,000 chemical synapses.

In this study we analyzed signed motif distributions in the *C. elegans* connectome using the connectome-scale synaptic polarity data published previously. We developed a novel method and computational tool to allow edge-labelled motif analysis and implemented it on the signed chemical synapse neuronal network of *C. elegans.* We carried out structure-preserving network randomization to generate null-models for motif analysis. We showed that some of the signed three-node motifs (most importantly negative feedback and positive feed-forward loops) are significantly overrepresented in the *C. elegan*s connectome.

Results

Induced subgraph analysis

The chemical synapse connectome of *C. elegans* consists of 3,638 connections of which 1,555, 553, and 1,530 were labeled as excitatory, inhibitory, or unknown, respectively, based on our previous work (14) and labelling detailed in Methods (Supplementary Data S1). In this network, we identified 64,962 individual three-node subgraphs (Supplementary Data S3). These subgraphs were categorized by their wiring structure and edge labelling into one of 710 unique motif types (Supplementary Data S2). To establish a null model, we generated a set of 1,000 networks by randomizing the neurotransmitter expression of the neurons. This resulted

in a varying ratio of excitatory and inhibitory connections amongst the random networks (Fig S1), but the total number and structure of edges remained the same across all networks. This set of random networks had on average fewer positive connections and more unknown connections than the original *C. elegans* connectome (Fig S1). We counted the occurrence of these motifs in the connectome and in the set of random networks and calculated Z-scores for each motif to determine over- or underrepresentation (Supplementary Data S4). We found 65 over- and 21 underrepresented motifs, respectively. Six motifs were absent both in the *C. elegans* connectome and in the null model, thus no Z-score was calculated. 184 motifs were only absent from the connectome. 38 of the overrepresented and 1 of the underrepresented motifs had no unknown edge, respectively (Fig S2).

Fig S1: **Distribution of different edge polarities among the connectome (crosses) and the generated 1 000 random networks (violin plots).** Random networks were generated by randomising the neurotransmitter expression of the neurons in the connectome, therefore only edge polarities have changed, the number of edges and nodes remained the same.

Fig S2: Induced motif analysis of the connectome. Using 1,000 random networks as a null-model, induced motif analysis revealed 38 significantly over- and 1 underrepresented motifs that have no unknown edge.

Partial subgraph analysis

Partial subgraph analysis can provide a deeper and more functional understanding of information processing networks (4,5). Therefore, we translated our findings of induced motifs to partial motif counts (Methods) and described 193,487 partial motifs in the connectome. We identified 92 significantly over- and 32 underrepresented partial motifs (Fig

2A, Supplementary Data S5). One motif (Motif A16) was absent both in the *C. elegans* connectome and in the null model, thus no Z-score was calculated. On the other hand, 22 motifs were only absent from the connectome. 40% of the identified partial motifs only had excitatory and inhibitory edges (Fig 2B). 56 of the significantly overrepresented and 1 of the significantly underrepresented motifs had no unknown edge, respectively (Fig 2C). Partial motifs with the highest Z-scores were characteristic for having one (but only one) inhibitory connection that provided negative feedback function in the motif.

Fig 2. Results of partial motif analysis. A) Distribution of all possible 710 signed three-node motifs. Over- and underrepresentation was determined in comparison to 1,000 random networks by using Z-score as quantitative measure. B) Distribution partial motifs of the connectome by the presence or absence of unknown edges. C) Significantly over- and underrepresented partial motifs (without unknown edge), and their respective Z-scores.

Previous studies (15) have shown the overrepresentation of symmetrical three-node motifs with a bidirectional edge (labelled in our work as motifs E and G). We found that only 8 of the possible 20 colourings of these motifs are significantly overrepresented (Fig 2C). Surprisingly, even though the structure of motifs E and G are symmetrical, 5 of the 8 overrepresented motifs are found to be asymmetrical in colouring.

Feedforward and feedback loops

We analyzed feedforward and feedback motifs in detail since they are known to be important in signalling networks (Table 1, references (16–23)). We differentiated eight types of feedforward and four types of feedback loops (Fig 3A), following previously published concepts (6,21).

148

149 Table 1.

	Motif	Type	Function	References
Feedback	D1	Positive	Amplification, information processing	18
	D2	**Negative**	**Oscillator, stabilizing**	**18**
	D3	**Disinhibitory (positive)**	**Amplification, creating a dense response**	**19, 20**
	D4	Oscillatory (negative)	Biological repressilator, oscillator	18, 21
Feedforward	**F1**	**Coherent positive**	**Sign-sensitive delay / persistance detector / learning; overrepresented in many systems**	**22, 23**
	F2	**Incoherent**	**Pulse generator, sign-sensitive accelerator.**	**23**
	F3	Incoherent	Pulse generator, sign-sensitive accelerator.	23
	F4	Coherent negative	Sign-sensitive delay	23
	F5	**Incoherent**	**Pulse generator, response accelerator, fold-change detection in sensory systems, input normalization; overrepresented in many systems**	**23, 24**
	F6	Coherent disinhibitory	Sign-sensitive delay, epileptic seisures	23, 25
	F7	Coherent negative	Sign-sensitive delay	23
	F8	Incoherent	Pulse generator, sign-sensitive accelerator	23

150 **Table 1. Feedback and feedforward signed motifs**. Motifs in **bold** are significantly

151 overrepresented in the *C. elegans* connectome.

152

153 **Fig 3. Feedforward and feedback motifs.** A) Feedforward and feedback motif counts in the

154 connectome (red X) compared to the null model of random networks (boxplot). Positive

155 feedback (Pos.), negative feedback (Neg.), disinhibitory feedback (Disinh.), oscillatory

156 feedback (Oscil.), positive feedforward, negative feedforward and incoherent feedfoward

157 loops are shown. The threshold of Z-score for significance was 1.96. B) Distribution of

158 significant feedback and feedforward motifs by neuron modality layouts. Neuron modalities

159 were abbreviated as S (sensory neuron), I (interneuron), and M (motor neuron). Layouts

160 containing at least one polymodal neuron (i.e. neuron without one specific modality) were
161 combined and labelled as P.
162
163 Addressing feedforward loops (Fig 3B), we found that the F1 coherent positive feedforward
164 and the F2 and F5 incoherent feedforward loops were overrepresented (Z-scores 3.09, 3.09,
165 and 4.18, respectively). The F1 motif was also the most abundant feedforward loop (2,167
166 occurrences). Meanwhile, the D2 negative feedback (Z-score = 5.14) and the D3 feedback
167 disinhibition (Z-score = 4.54) loops were also highly overrepresented. Positive feedback (D1)
168 and coherent negative feedforward (F4, F7) loops were not overrepresented.
169 In the next step, we further analyzed the neuron modality (i.e. sensory, motor, inter,
170 polymodal) distributions amongst the significant feedforward and feedback loops. We found
171 a pattern that specific modality layouts (numbered 1 to 27, excluding polymodal-containing
172 motifs) dominated each feedforward motif (Fig 3D). In case of the F1 coherent positive
173 feedforward loop, the most common modality layout was #21, which represents inter->motor
174 and motor->motor excitation. For the F2 ('incoherent') motif the dominant modality layout
175 was #10 which represents inter->inter inhibition and inter->motor excitation pattern. For the
176 F5 (also 'incoherent') motif the dominant layout was #15 which is a sensory->inter excitatory
177 and inter->inter inhibitory layout. We observed that the interneuron-only layout (#3) was
178 equally the second most frequent layout amongst all three overrepresented feedforward
179 motifs.
180
181 In case of feedback loops (Fig 3C, both the D2 negative feedback and the D3 disinhibitory
182 loops were highly present in the interneuron-only layout (#3). On the other hand, the D3
183 feedback loop was also found to be dominant in modality layout #21 (which is representing
184 inter->motor excitation, motor->motor inhibition, and motor->inter inhibition), while the D2

was not. Surprisingly, we did not observe a single occurrence of an archetypical three-layer negative feedback loop (i.e. layout #22: sensory->inter and inter->motor excitation, and motor->sensory inhibition). Modality layouts having at least one polymodal neuron were highly frequent in the case of all motifs but were presented as a single layout to simplify interpretation.

Discussion

The neuronal network of *C. elegans* is yet the only fully reconstructed connectome (10) which allows detailed analysis to comprehend the structural characteristics such as network motif abundance of a nervous system. Utilizing the previously published signed connectome of *C. elegans* we conducted signed motif analysis for the first time, to our knowledge. We found that the previously reported high number of feedforward loops (15) is disproportionately distributed among the different edge colouring patterns. The coherent excitatory feedforward loop and two types of incoherent feedforward loops are overrepresented compared to random networks. The incoherent feedforward loops are overrepresented in many systems (3,24) and function as sign-sensitive accelerators which have key roles in information processing of networks (21). The role of the negative feedback loop is also highly overrepresented in the *C. elegans* connectome and is well-known in various networks (25,26). We also found overrepresentation of the disinhibitory feedback motif which has a more complex function: it plays an important role in balancing excitation and inhibition in a signed network. It can lead to novelty response amplification and a dense population response (18). It was found in the primary visual cortex (27) and in the nucleus accumbens regulating aversion and reward (17). Having two different steady states (6), a disinhibitory feedback motif can act as a biological switch (28).

There are several limitations of our study. Because of the limited data available, we were only able to analyze 40% of all three-node motifs of the connectome (graphlets having only excitatory or inhibitory function in the network). New connectivity data of the worm are still emerging (29,30) and there are recent experimental results of synaptic polarity and gene expression as well (31). However, the relatively high number of complex connections (14) implies that our results can be complemented once the role of those synapses is better understood.

Overall, to our knowledge, our study provides the first comprehensive analysis of signed motifs in a fully mapped connectome, revealing insights into the functional architecture of the *C. elegans* neuronal network. The overrepresentation of certain motif types, particularly positive feedforward and negative feedback loops, suggests that these motifs likely contribute significantly to the network's information processing and homeostatic functions. Future work that incorporates emerging synaptic polarity data and expands beyond three-node motifs could yield even deeper insights into the organizational principles of neural networks. As motif analysis techniques evolve and are applied to larger-scale connectomes, our findings offer a foundation for exploring how distinct motif configurations support the complex functions of diverse nervous systems.

Materials and Methods

Description of the *C. elegans* connectome data

The WormWiring connectome reconstruction (http://wormwiring.org) of the adult hermaphrodite worm consists of 3,638 chemical connections (20,589 synapses) connecting 297 neurons (CANL, CANR, PLML, PLMR, and M5 neurons are not connected by chemical connections hence were excluded from the analysis). We utilized the signed neuronal

network published previously in which synaptic signs were predicted based on cellular level neurotransmitter and receptor expression data (14). In the original work synapses were predicted as excitatory, inhibitory, complex, or unknown. In the current work complex synapses were re-labelled as excitatory, inhibitory, or unknown, based on the balance of postsynaptic receptor expression (e.g. connections that had excitatory>inhibitory postsynaptic receptors were defined as positive) to reduce combinatorial complexity, similarly to a method used previously (32). Hence, in this work a network edge was coloured with one of three labels (Supplementary Data S1). We extracted neuron modalities (i.e. sensory, inter, motor, or polymodal) from Wormatlas (http://wormatlas.org). Neurons with more than one functional modality (e.g. inter and motor), were labelled as polymodal.

Definition and search of signed motifs

A definition system of directed and edge-coloured motifs consisting of three nodes was established. Edges were signed as either excitatory, inhibitory or unknown, resulting in 710 motifs (Supplementary Data S2). Rotational and reflectional symmetries were considered as the same motif. Motif search was performed by a self-developed algorithm (https://github.com/bank-fenyves/CeConn-ColorMotifs) that seeks for induced subgraphs, identifies all three-node, edge-coloured motifs in the target network, and categorizes them as one of the 710 motif types. Our algorithm was further used to convert induced motif counts to partial motif counts.

Randomization and statistical analysis

Generation of random networks was performed by shuffling neurotransmitter expression of the neurons and then predicting synaptic polarities repeatedly. Thus, the structural hard-wiring of the random networks were preserved. This allowed us to use absolute motif counts

for analysis. 1,000 random networks were generated which were used as a null model. In formal analysis we tested the alternative hypothesis that a coloured motif in the *C. elegans* neuronal network is significantly over- or underrepresented compared to the null model, as established previously (13). As an established method to assess statistical significance of individual motifs (3,33). Z-score was computed, using a threshold of |Z-score| = 1.96, corresponding to a 95% confidence interval (alpha=0.05). For each motif Z-score was calculated using the formula:

$$Z = \frac{f_{conn} - f_{rand}}{std(f_{rand})}$$

where f_{conn} is the frequency of the motif in the connectome, f_{rand} is the average frequency of the motif in the random networks, while $std(f_{rand})$ stands for the standard deviation of the motifs occurence in random networks.

Software

The motif search algorithm was developed in Python (3.10.11). Randomization of the network and polarity prediction was performed in R (4.2.2). Statistical tests were performed in R (4.2.2) and Microsoft Excel (16.84). All scripts are available at https://github.com/bank-fenyves/CeConn-ColorMotifs.

Acknowledgements

The authors thank Istvan Kovacs (Northwestern University, Department of Physics and Astronomy) and Balazs Hangya (HUN-REN Institute of Experimental Medicine) for meaningful discussions, and all members of the LINK group for their inputs.

References

1. Bassett DS, Bullmore ET. Small-world brain networks revisited. Vol. 23, *Neuroscientist*. SAGE Publications Inc.; 2017. p. 499–516.
2. Bullmore E, Sporns O. Complex brain networks: graph theoretical analysis of structural and functional systems. Nat Rev Neurosci. 2009 Mar 4;10(3):186–98.
3. Milo R, Shen-Orr S, Itzkovitz S, Kashtan N, Chklovskii D, Alon U. Network Motifs: Simple building blocks of complex networks. Science (1979). 2002 Oct 25;298(5594):824–7.
4. Sporns O, Kötter R. Motifs in brain networks. PLoS Biol. 2004 Oct 26;2(11):e369.
5. McDonnell MD, Yaveroğlu ÖN, Schmerl BA, Iannella N, Ward LM. Motif-Role-Fingerprints: The building-blocks of motifs, clustering-coefficients and transitivities in directed networks. PLoS One. 2014 Dec 8;9(12):e114503.
6. Alon U. Network motifs: theory and experimental approaches. Nat Rev Genet. 2007 Jun;8(6):450–61.
7. Mason MJ, Valente TW, Coatsworth JD, Mennis J, Lawrence F, Zelenak P. Place-based social network quality and correlates of substance use among urban adolescents. J Adolesc. 2010 Jun 8;33(3):419–27.
8. Park B yong, Hong SJ, Valk SL, Paquola C, Benkarim O, Bethlehem RAI, et al. Differences in subcortico-cortical interactions identified from connectome and microcircuit models in autism. Nat Commun. 2021 Apr 13;12(1):2225.
9. Varshney LR, Chen BL, Paniagua E, Hall DH, Chklovskii DB. Structural properties of the *Caenorhabditis elegans* neuronal network. PLoS Comput Biol. 2011 Feb 3;7(2):e1001066.

10. White JG, Southgate E, Thomson JN, Brenner S. The structure of the nervous system of the nematode *Caenorhabditis elegans*. Philosophical Transactions of the Royal Society of London B, Biological Sciences 1986 Nov 12;314(1165):1–340.

11. Matejek B, Wei D, Chen T, Tsourakakis CE, Mitzenmacher M, Pfister H. Edge-colored directed subgraph enumeration on the connectome. Sci Rep. 2022 Jul 5;12(1):11349.

12. Pereira L, Kratsios P, Serrano-Saiz E, Sheftel H, Mayo AE, Hall DH, et al. A cellular and regulatory map of the cholinergic nervous system of C. elegans. Elife. 2015 Dec 25;4:e12432.

13. Qian J, Hintze A, Adami C. Colored motifs reveal computational building blocks in the *C. elegans* brain. PLoS One. 2011 Mar 7;6(3):e17013.

14. Fenyves BG, Szilágyi GS, Vassy Z, Sőti C, Csermely P. Synaptic polarity and sign-balance prediction using gene expression data in the *Caenorhabditis elegans* chemical synapse neuronal connectome network. PLoS Comput Biol. 2020 Dec 21;16(12):e1007974.

15. Reigl M, Alon U, Chklovskii DB. Search for computational modules in the *C. elegans* brain. BMC Biol. 2004;2(1):25.

16. Cinquin O, Demongeot J. Positive and negative feedback: Striking a balance between necessary antagonists. J Theor Biol. 2002;216(2):229–41.

17. Liu Z, Le Q, Lv Y, Chen X, Cui J, Zhou Y, et al. A distinct D1-MSN subpopulation down-regulates dopamine to promote negative emotional state. Cell Res. 2022 Feb 1;32(2):139–56.

18. Schulz A, Miehl C, Berry MJ, Gjorgjieva J. The generation of cortical novelty responses through inhibitory plasticity. Elife. 2021 Oct 1;10.

19. Elowitz MB, Leibler S. A synthetic oscillatory network of transcriptional regulators. Nature. 2000 Jan;403(6767):335–8.

20. Keifer J, Houk JC. Modeling Signal Transduction in classical conditioning with network motifs. Front Mol Neurosci. 2011;4.

21. Mangan S, Alon U. Structure and function of the feed-forward loop network motif. Proceedings of the National Academy of Sciences. 2003 Oct 14;100(21):11980–5.

22. Goentoro L, Shoval O, Kirschner MW, Alon U. The incoherent feedforward loop can provide fold-hange detection in fene regulation. Mol Cell. 2009 Dec 11;36(5):894–9.

23. Birjandian Z, Narla C, Poulter MO. Gain control of γ frequency activation by a novel feed forward disinhibitory loop: Implications for normal and epileptic neural activity. Front Neural Circuits. 2013 Nov 19;7(NOV).

24. Shen-Orr SS, Milo R, Mangan S, Alon U. Network motifs in the transcriptional regulation network of Escherichia coli. Nat Genet. 2002 May 22;31(1):64–8.

25. Krishna S. Structure and function of negative feedback loops at the interface of genetic and metabolic networks. Nucleic Acids Res. 2006 Apr 28;34(8):2455–62.

26. Yan Q, Zhu K, Zhang L, Fu Q, Chen Z, Liu S, et al. A negative feedback loop between JNK-associated leucine zipper protein and TGF-β1 regulates kidney fibrosis. Commun Biol. 2020 Dec 1;3(1).

27. Keller AJ, Dipoppa M, Roth MM, Caudill MS, Ingrosso A, Miller KD, et al. A disinhibitory circuit for contextual modulation in primary visual cortex. Neuron. 2020 Dec;108(6):1181-1193.e8.

28. Gardner TS, Cantor CR, Collins JJ. Construction of a genetic toggle switch in *Escherichia coli*. Nature. 2000 Jan;403(6767):339–42.

29. Witvliet D, Mulcahy B, Mitchell JK, Meirovitch Y, Berger DR, Wu Y, et al. Connectomes across development reveal principles of brain maturation. Nature. 2021 Aug 12;596(7871):257–61.

30. Emmons SW. Comprehensive analysis of the C. elegans connectome reveals novel circuits and functions of previously unstudied neurons. PLoS Biol 22(12): e3002939.

31. Zhang G, Roberto NM, Lee D, Hahnel SR, Andersen EC. The impact of species-wide gene expression variation on *Caenorhabditis elegans* complex traits. Nat Commun. 2022 Jun 16;13(1):3462.

32. Hardege I, Morud J, Courtney A, Schafer WR. A novel and functionally diverse class of acetylcholine-gated ion channels. Journal of Neuroscience. 2023 Feb 15;43(7):1111–24.

33. Xia F, Wei H, Yu S, Zhang D, Xu B. A survey of measures for network motifs. IEEE Access. 2019;7:106576–87.

Competing interests

The authors declare no competing interests.

Author contribution

G.S.S contributed to conception, design, developing the algorithm, analysis and wrote the manuscript; A.G. contributed to conception and analysis, Z.V. contributed to the interpretation of data; P.C. contributed to conception, interpretation of data, and to the manuscript. B.G.F. contributed to conception, data analysis, and to the manuscript.

Description of supplementary data

Supplementary Data S1: Polarity of edges in the connectome and random networks

Supplementary Data S2: Motif codes and dictionary

Supplementary Data S3: Motifs in the connectome

Supplementary Data S4: Induced motif counts and Z-scores in the connectome and in the null model

Supplementary Data S5: Partial motif counts and Z-scores in the connectome and in the null model

A

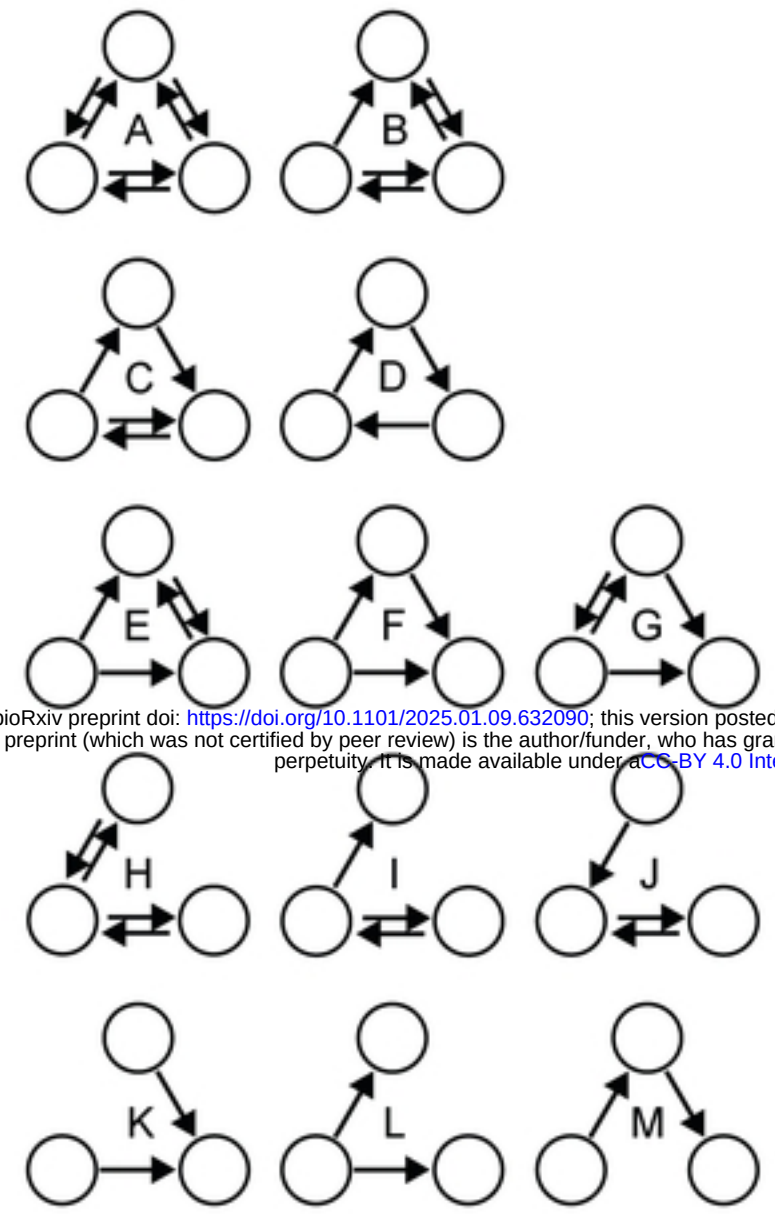

B

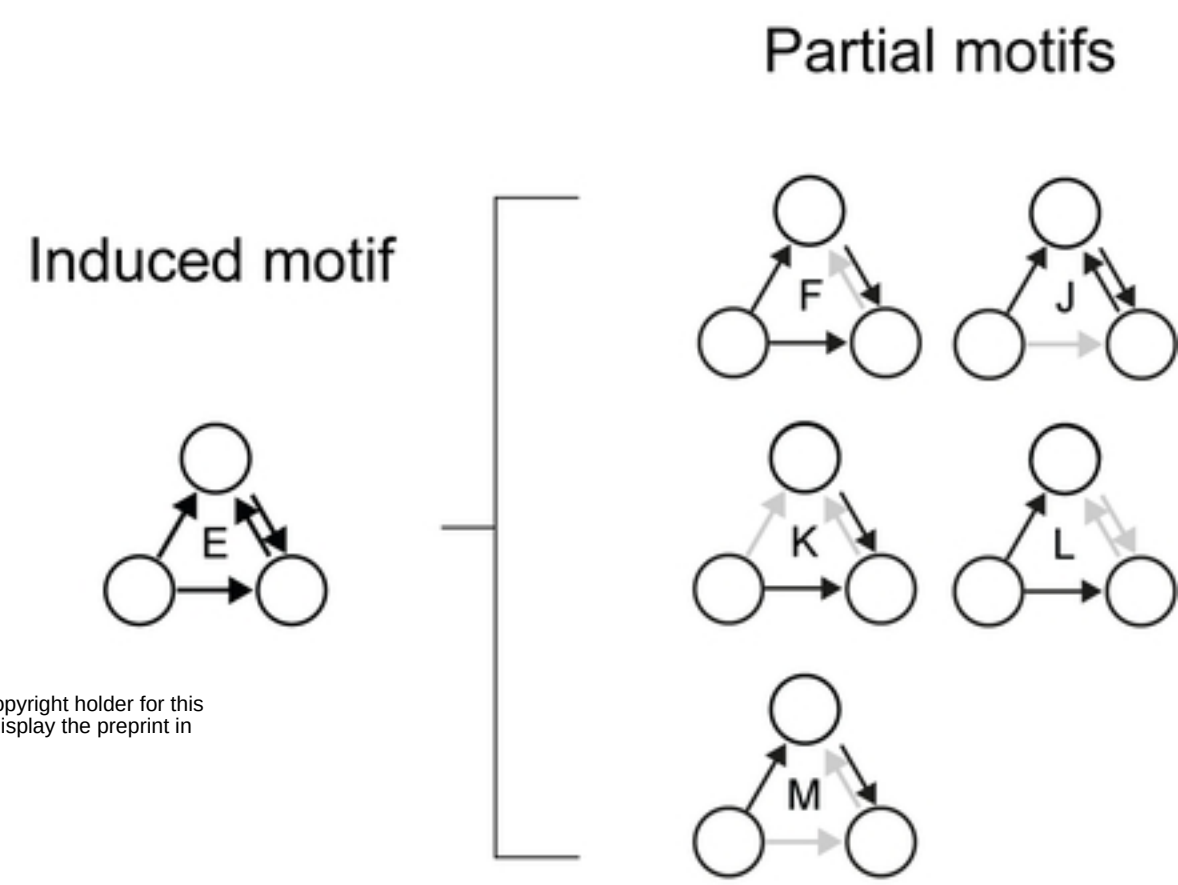

C

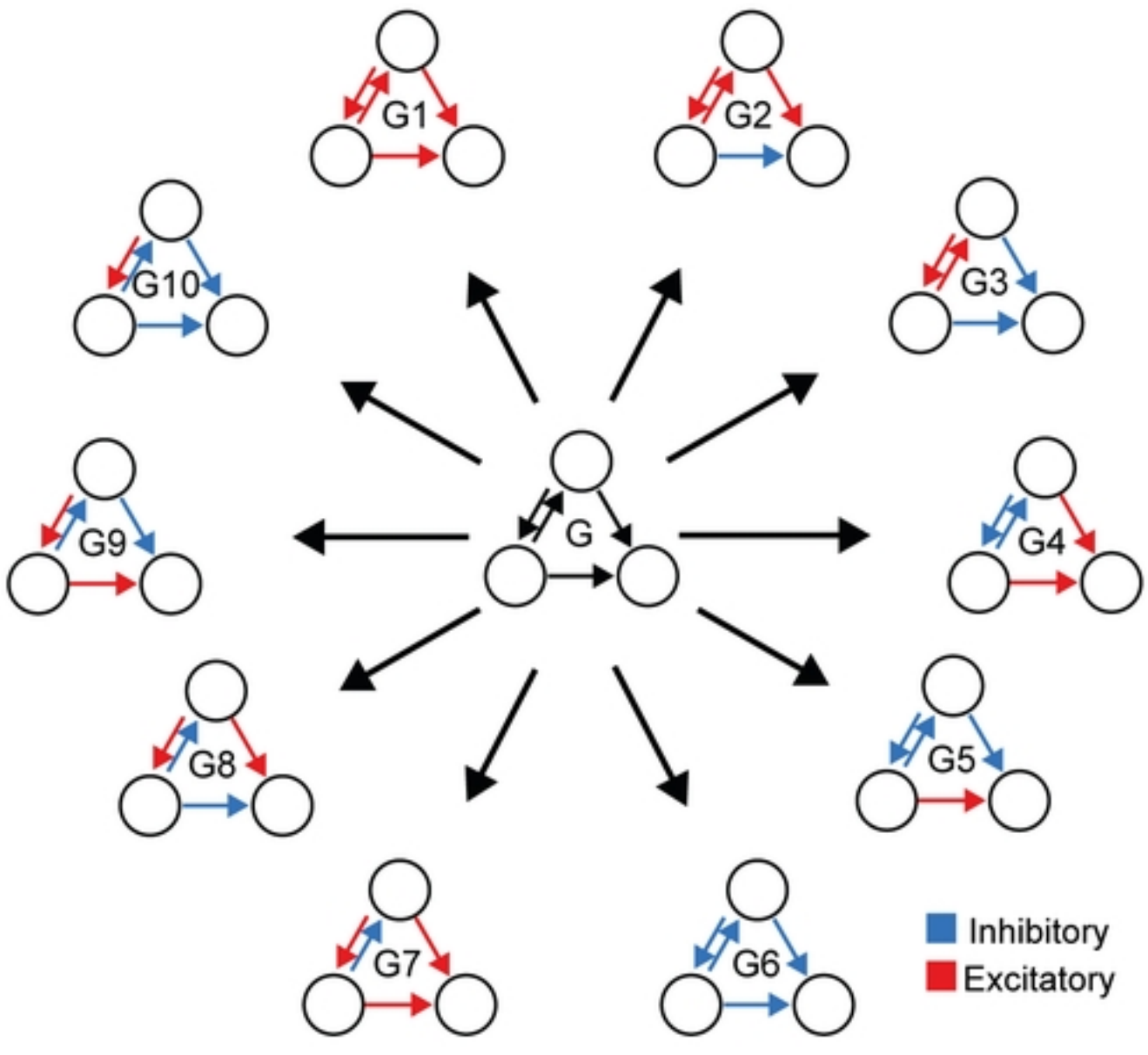

Figure 1

A

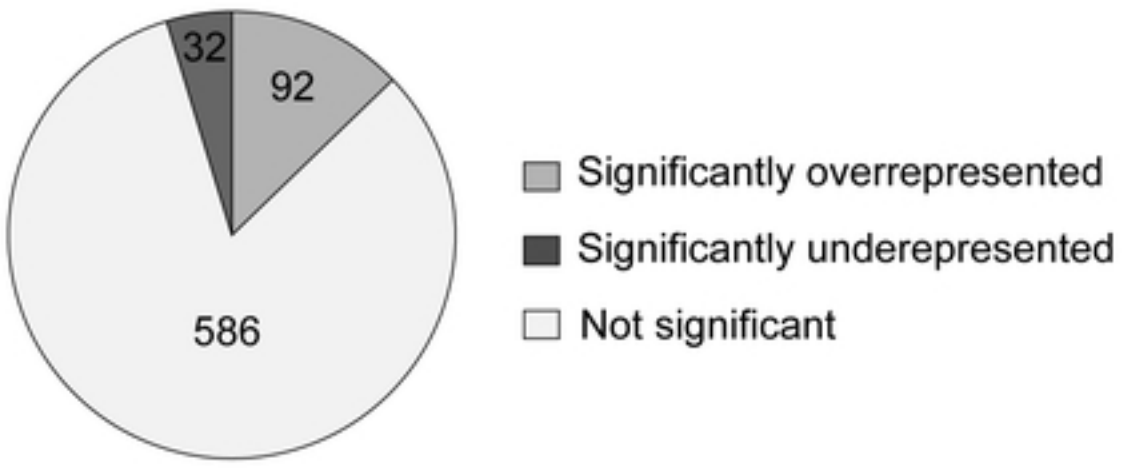

B

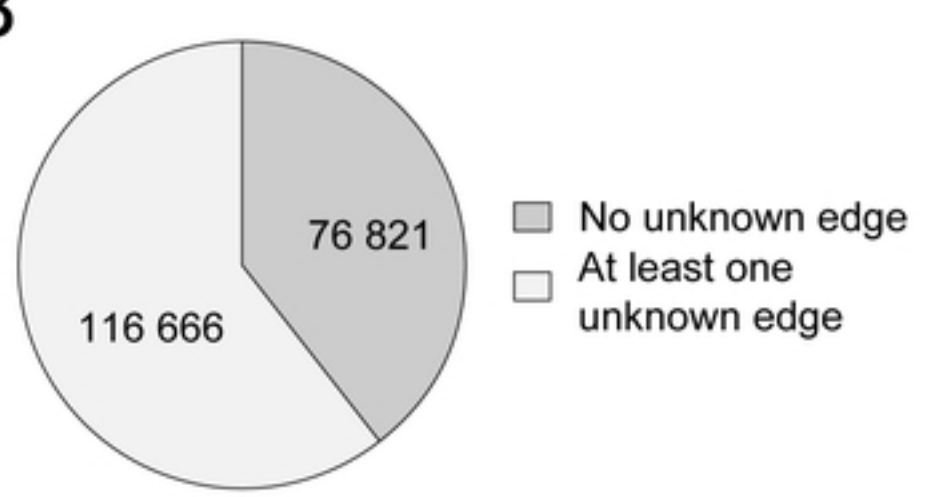

C

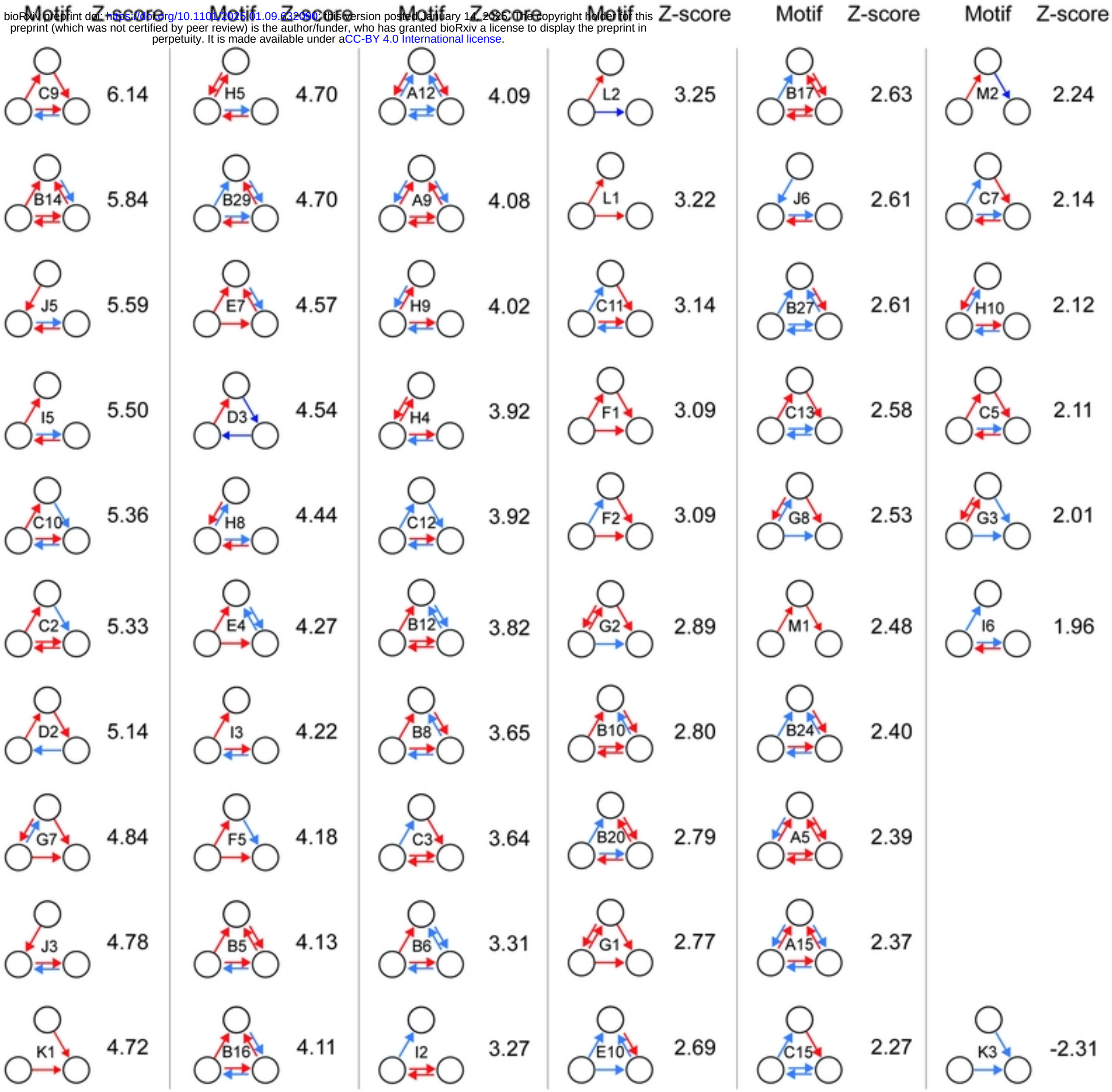

Figure 2

A

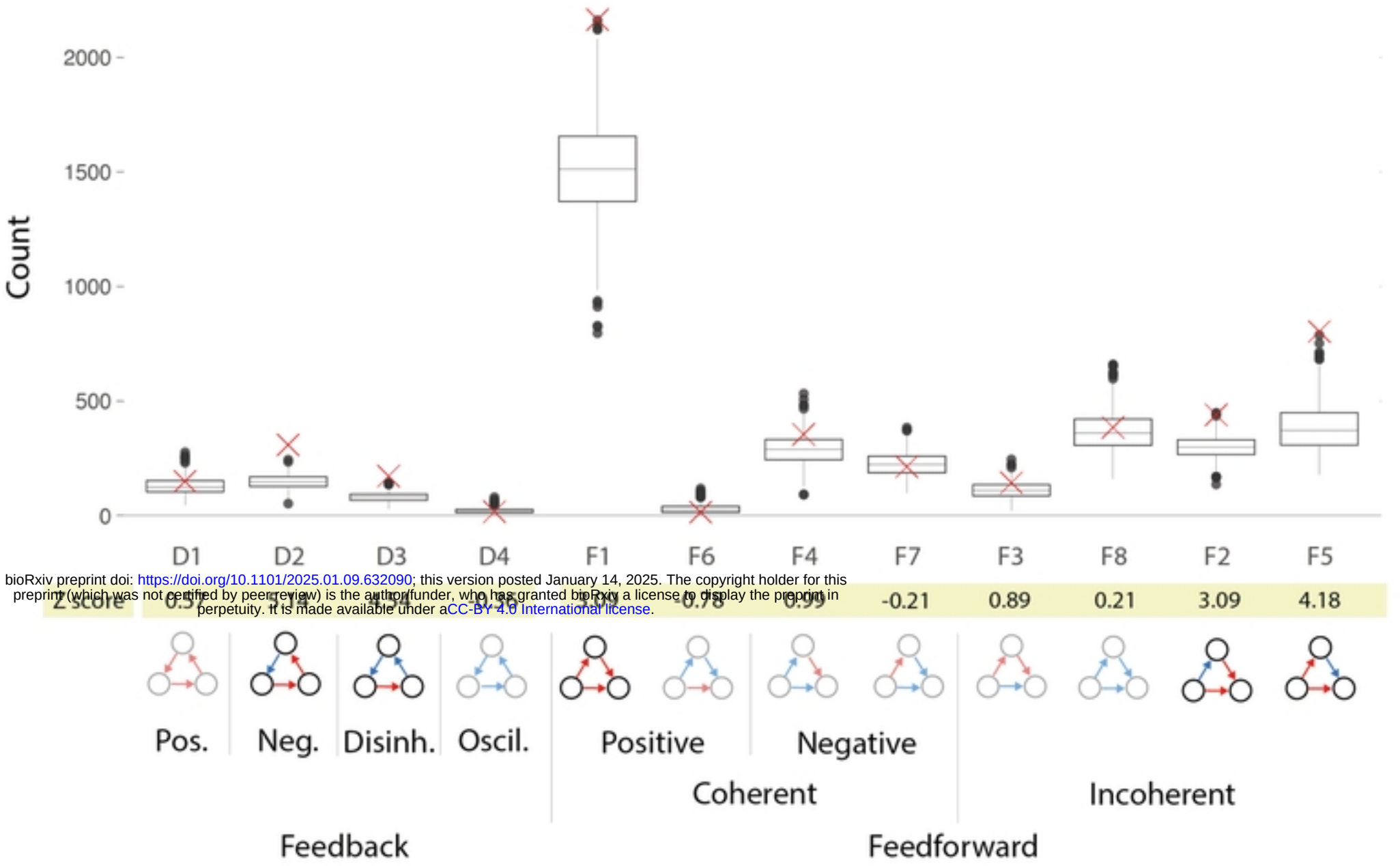

B

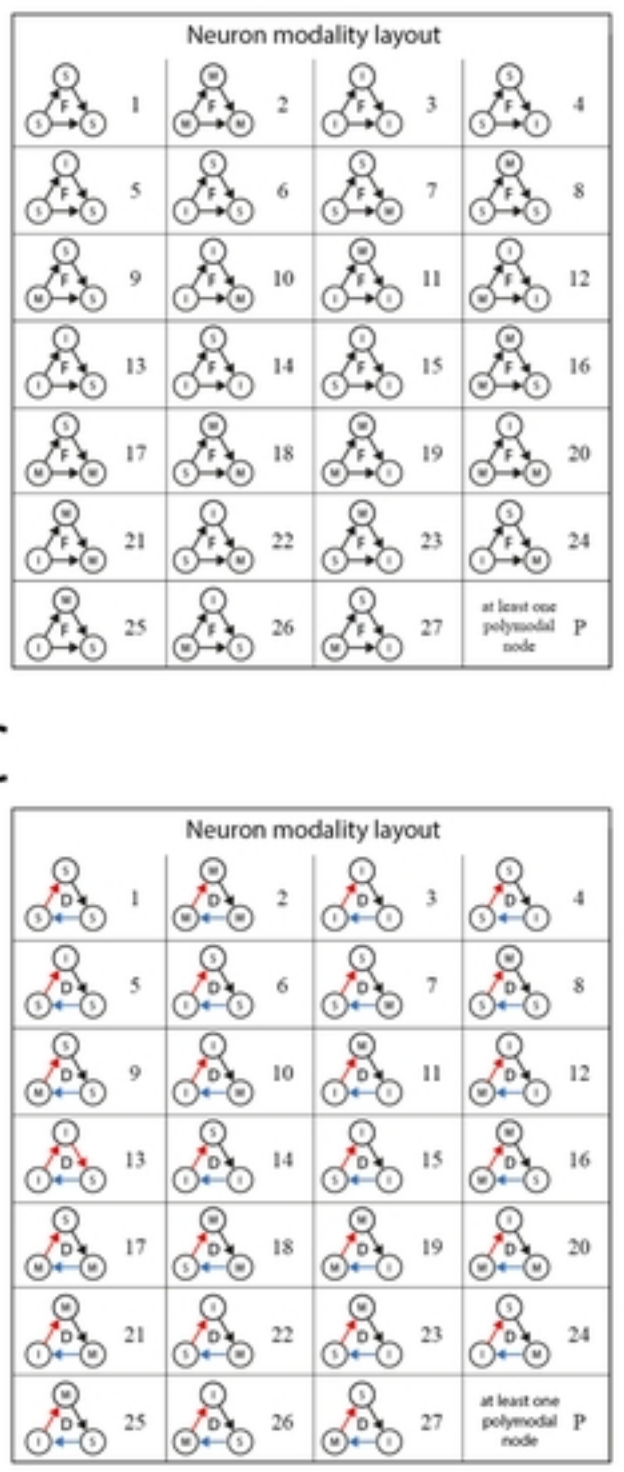

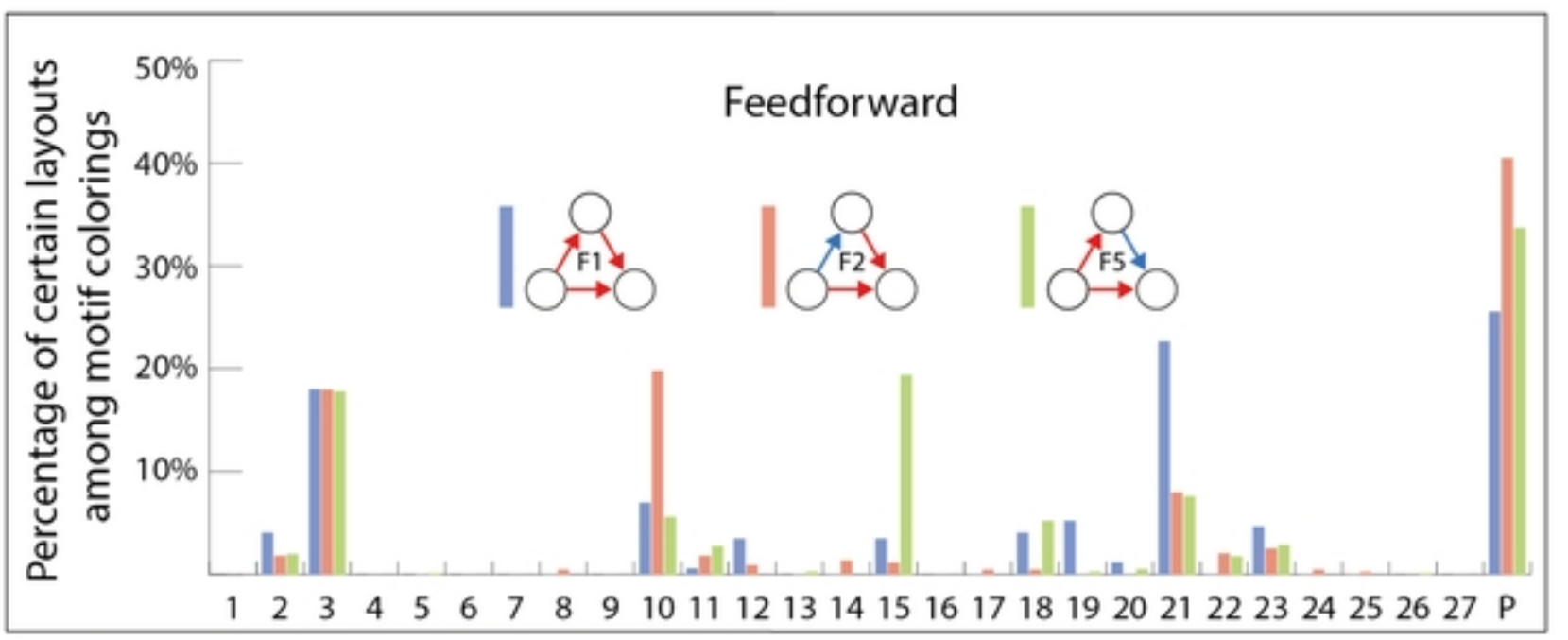

C

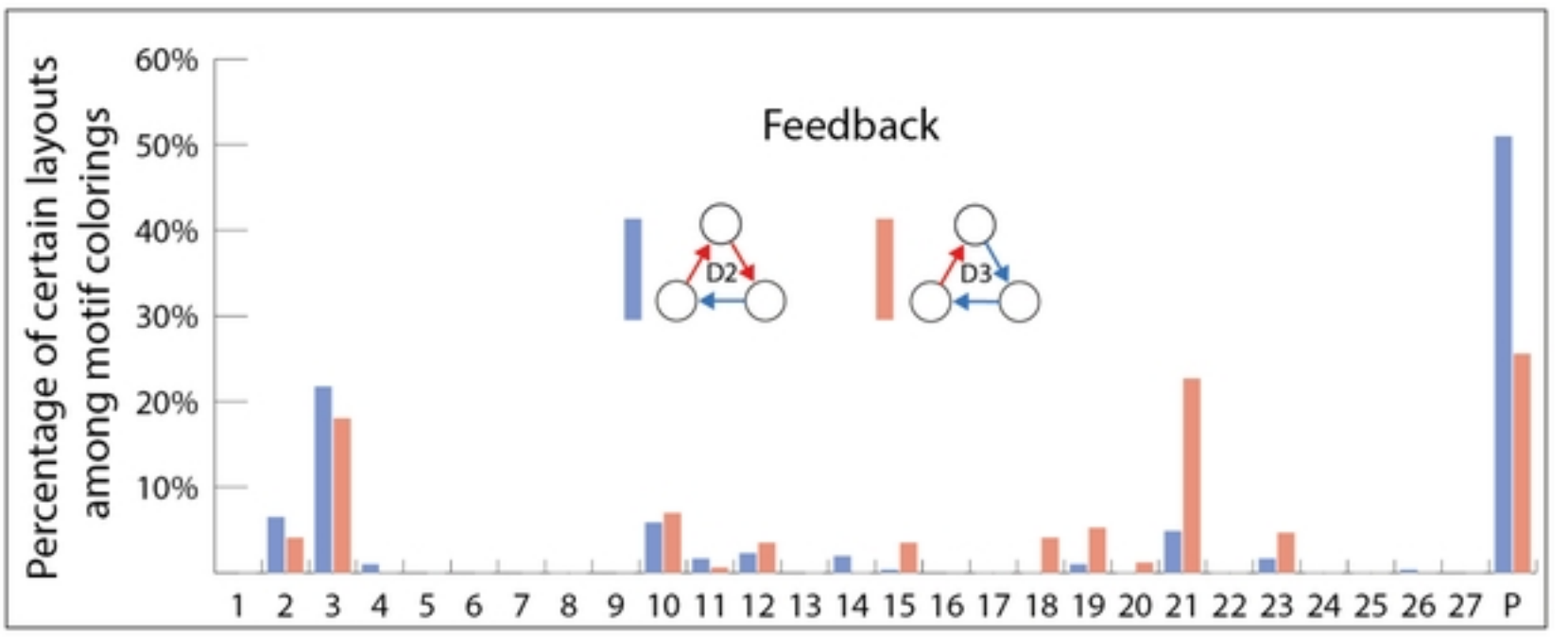

Figure 3

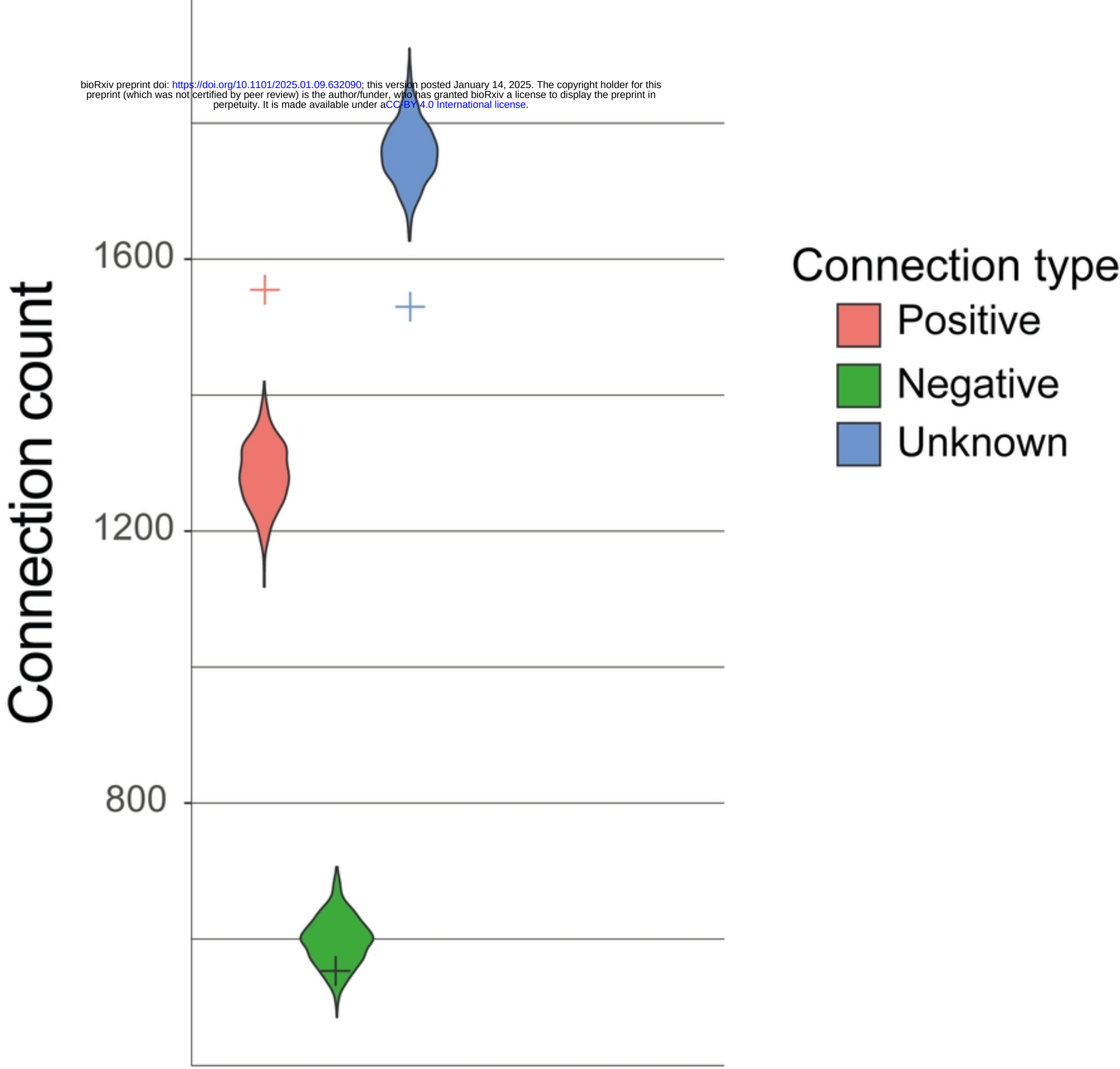

Figure S1

Motif	Z-score	Motif	Z-score	Motif	Z-score	Motif	Z-score
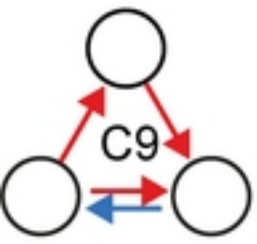	7.95	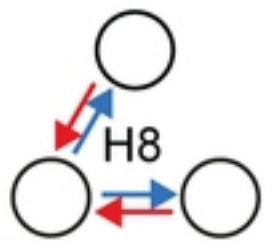	4.82	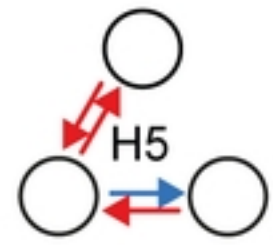	3.35	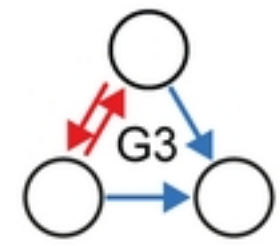	2.40
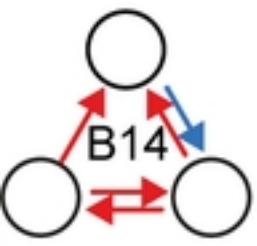	7.35		4.60	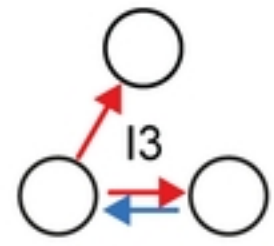	3.19	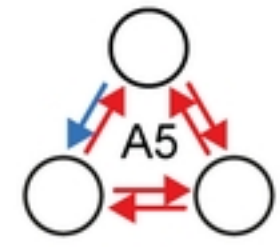	2.39
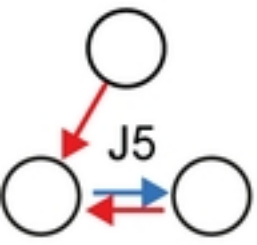	6.51	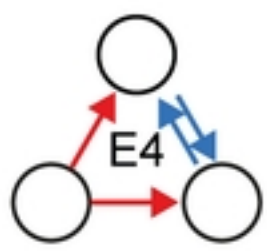	4.26	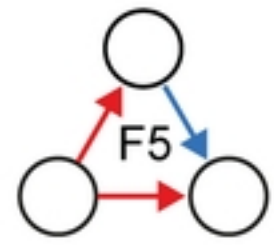	2.96	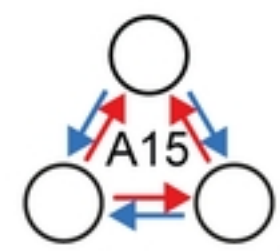	2.37
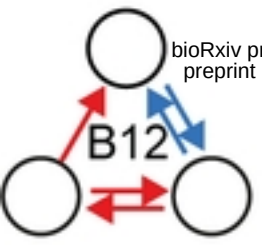	6.31	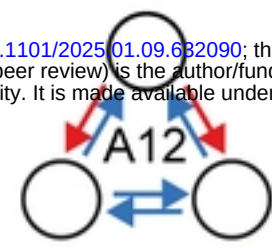	4.09	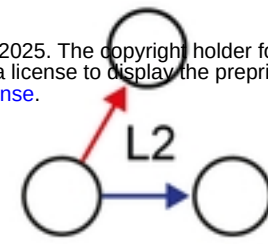	2.91	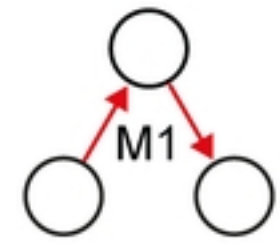	2.31
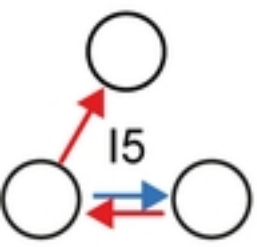	5.78	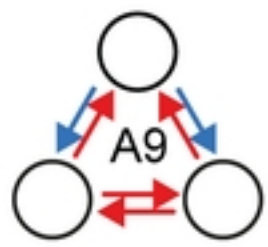	4.08	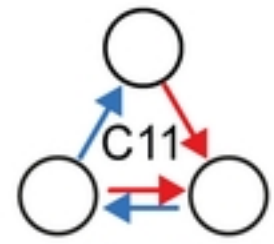	2.70	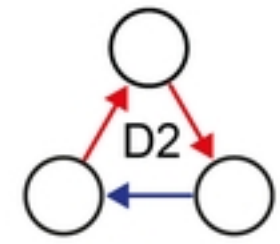	2.30
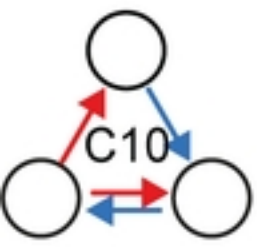	5.48	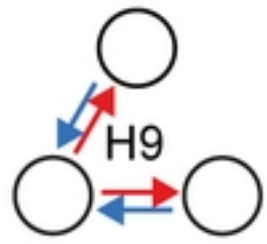	4.07	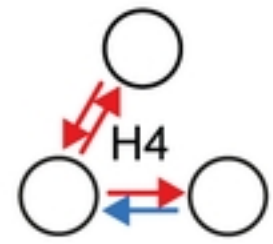	2.58	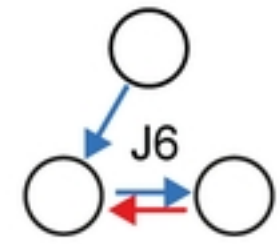	2.27
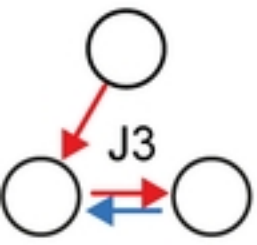	5.47	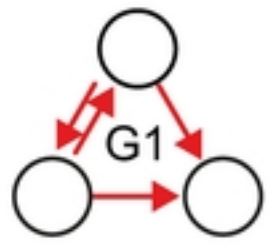	3.90	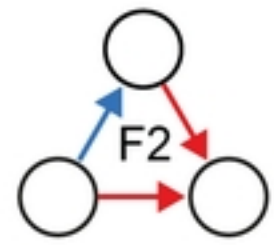	2.53	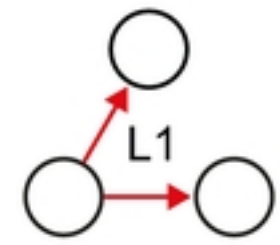	2.21
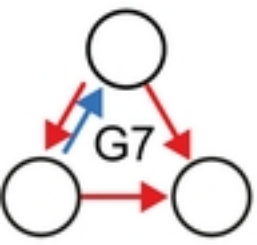	5.26	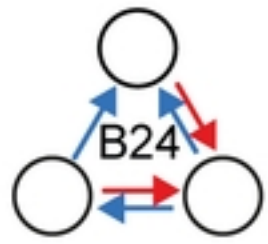	3.81	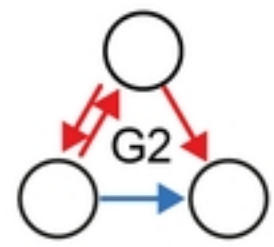	2.47	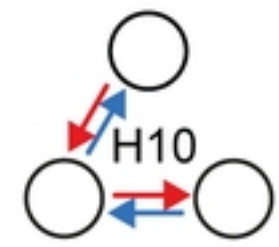	1.96
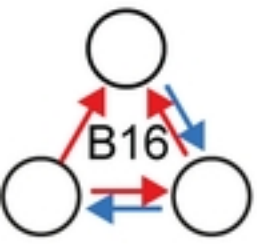	4.88	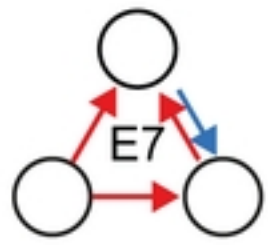	3.53	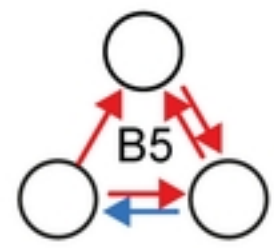	2.46		
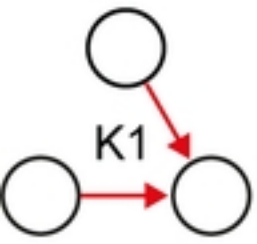	4.86	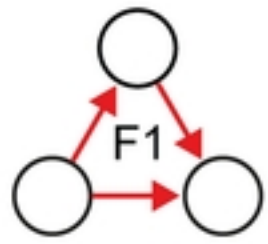	3.37	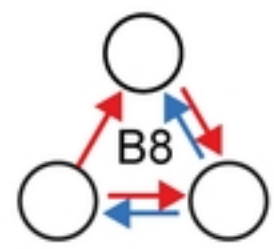	2.41	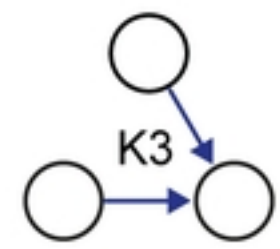	-3.29

Figure S2